Supporting Information

Nanoflower-like high-entropy Ni-Fe-Cr-Mn-Co (oxy)hydroxides for oxygen evolution

Mingyuan Shi[a,b], Tianmi Tang[b], Liyuan Xiao[b], Jingyi Han[b], Xue Bai[b], Yuhang Sun[a,b], Siyu Chen[b], Jingru Sun[b], Yuanyuan Ma[a,*], and Jingqi Guan[b,*]

[a] College of Chemistry and Chemical Engineering, Qiqihar University, Heilongjiang Province 161006, China. *E-mail: mayuanyuan1219@126.com (Y.Y. Ma)

[b] Institute of Physical Chemistry, College of Chemistry, Jilin University, 2519 Jiefang Road, Changchun 130021, P. R. China. *E-mail: guanjq@jlu.edu.cn (J.Q. Guan)

Synthesis of FeNiCrMnCoOOH/NF

Nickel NF foam (2 cm × 2 cm) was treated in 3 M HCl, distilled water and absolute ethanol for 15 min, respectively. Then, 0.404 g $Fe(NO_3)_3·9H_2O$, 0.291 g $Co(NO_3)_2·6H_2O$, 0.2326 g $Ni(NO_3)_2·6H_2O$, 0.32 g $Cr(NO_3)_3·9H_2O$, 0.136 g $MnSO_4·H_2O$, 0.24 g NH_2CONH_2 and 0.075 g PVP were dissolved in 20 mL of H_2O via ultrasonic treatment. Subsequently, the solution was transferred into a 25 mL Teflon autoclave and a processed piece of NF was added, which was heated at 100 °C for 12 hours. Finally, the obtained NF was washed three times with ethanol and distilled water and dried at 60 °C for 12 hours, which was nominated as

FeNiCrMnCoOOH/NF. For comparison, the quaternary FeNiCrMnOOH/NF, ternary FeNiMnOOH/NF, binary NiMnOOH/NF, unary NiOOH/NF and four other high-entropy (oxy)hydroxides FeNiCrMnAlOOH, FeNiCrMnCuOOH, FeNiCrMnMoOOH and FeNiCrMnCeOOH were synthesized following a process similar to that for FeNiCrMnCoOOH/NF.

Characterization

Powder X-ray diffraction (XRD) patterns were collected using a Shimadzu XRD-6000 with Cu Kα radiation (40 kV, 30 mA). HRTEM images were recorded on a JEM-2100 transmission electron microscope (Tokyo, Japan) at 200 kV. SEM images were recorded on a HITACHI SU8020 field emission scanning electron microscope. Raman spectra were acquired using a Renishaw micro-Raman spectrometer with a 532 nm laser at 0.2 mW. The valence state was determined using XPS recorded on a Thermo ESCALAB 250Xi. The X-ray source selected was monochromatized Al Kα source (15 kV, 10.8 mA). Region scans were collected using 30 eV pass energy. Peak positions were calibrated relative to C 1s peak position at 284.6 eV.

Electrochemical measurements

All electrochemical measurements were performed on a CHI760E electrochemical working station at room temperature. The catalysts were measured in 1 M KOH aqueous solution using a typical three-electrode configuration. Linear sweep voltammetry (LSV) polarization curves were acquired at a scan rate of 5 $mV \cdot s^{-1}$. Electrochemical impedance spectroscopy (EIS) measurements were performed at open-circuit potential in the frequency range from 100 kHz to 0.1 Hz with an a.c.

perturbation of 5 mV. All potentials measured were calibrated to RHE using the following equation: E (versus RHE) = E (versus SCE) + 0.241 V + 0.0591 pH.

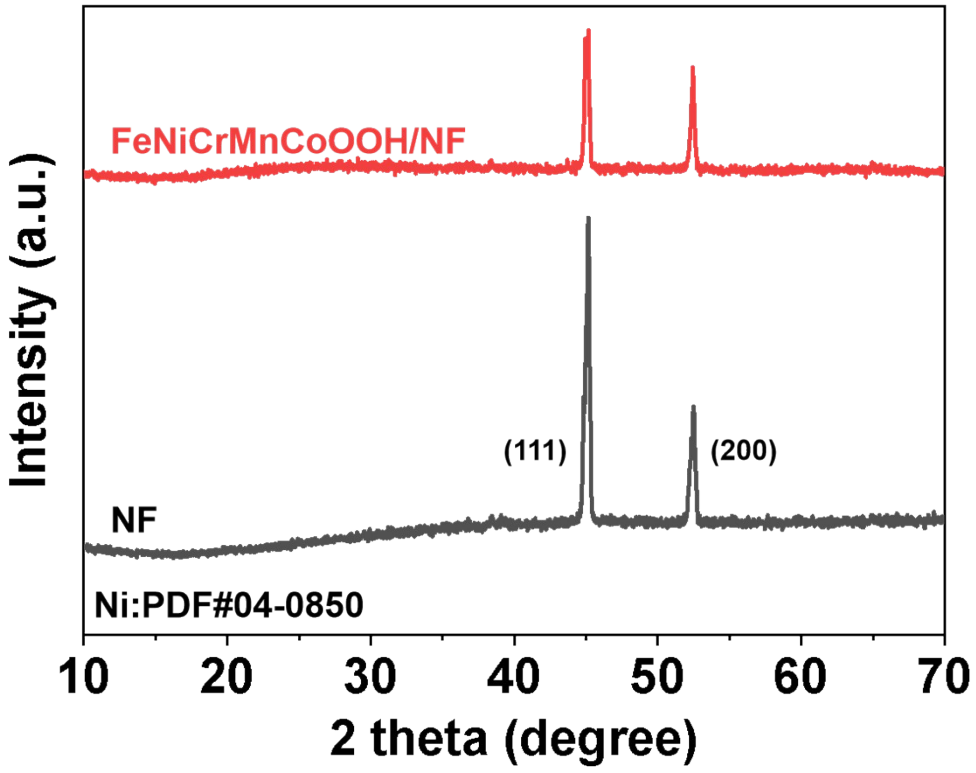

Fig. S1. XRD patterns of NF and FeNiCrMnCoOOH/NF.

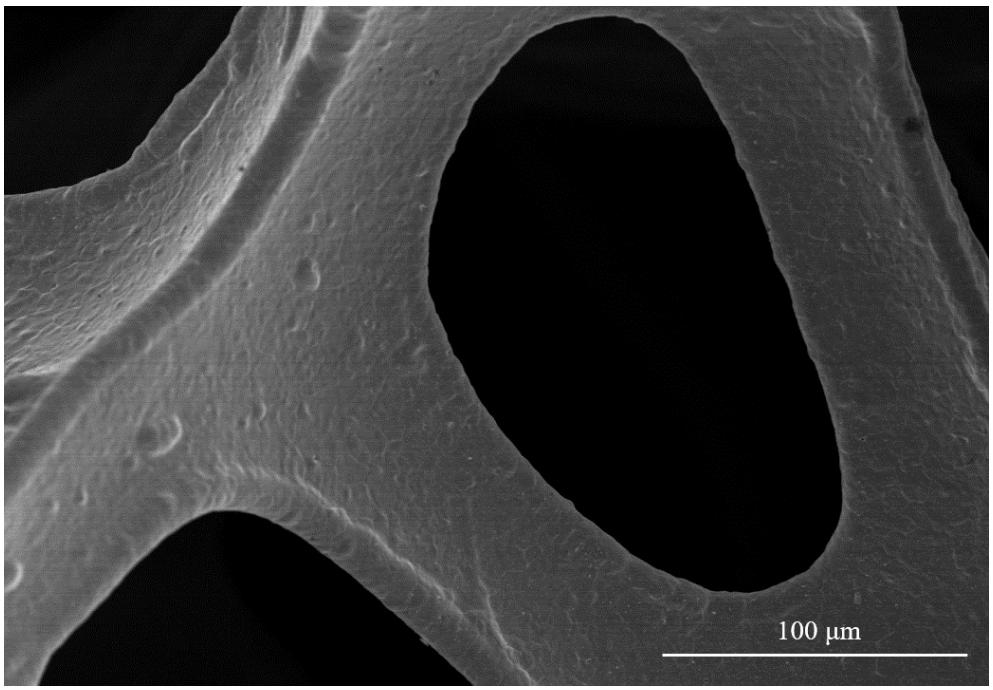

Fig. S2. SEM image of NF.

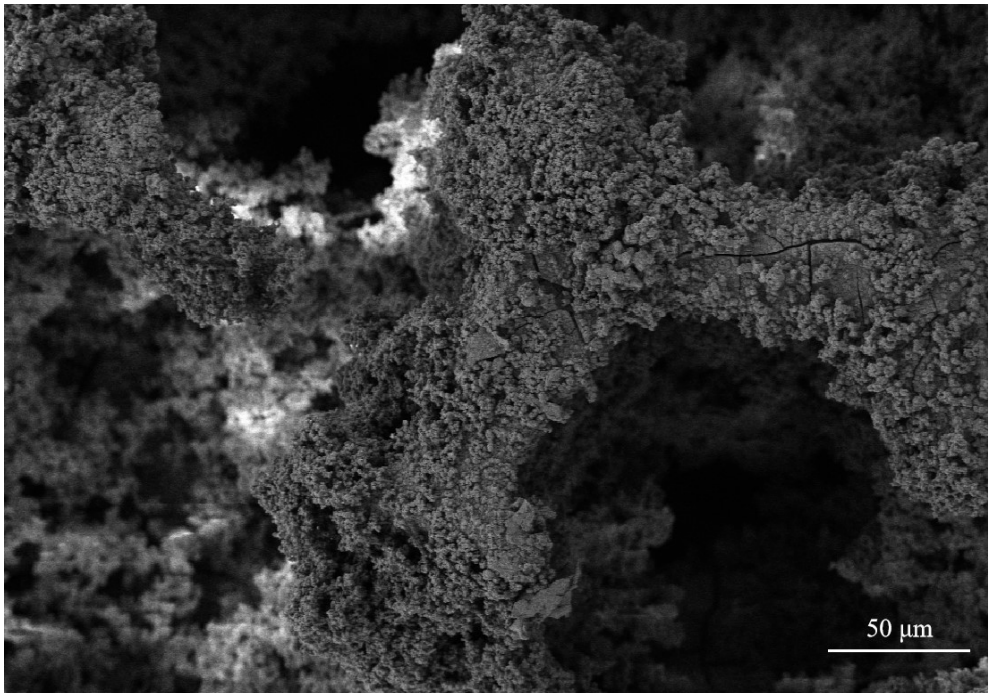

Fig. S3. SEM image of FeNiCrMnCoOOH/NF.

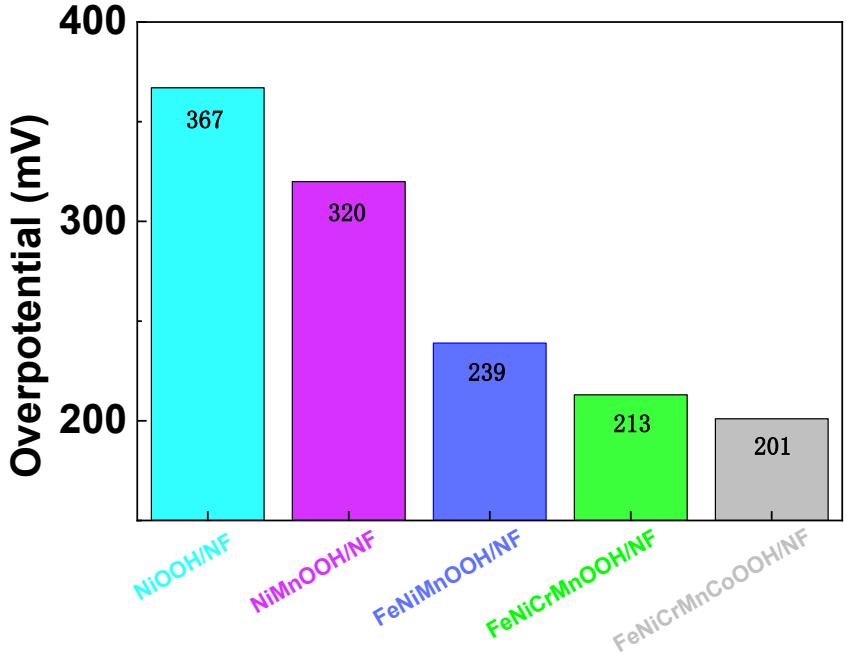

Fig. S4. Overpotential comparison at 10 mA cm^{-2}.

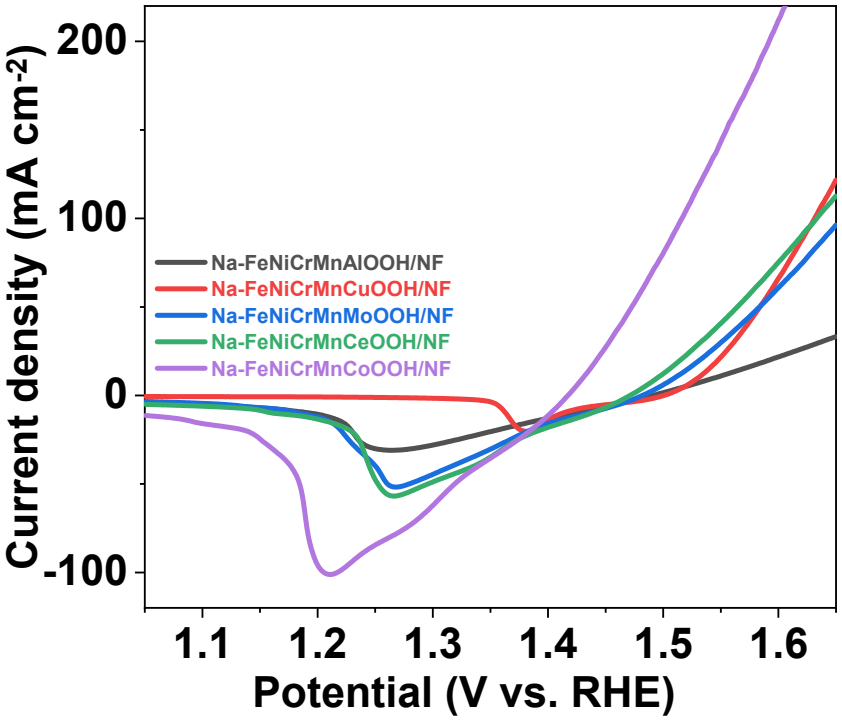

Fig. S5. LSV curves of FeNiCrMnAlOOH/NF, FeNiCrMnCuOOH/NF, FeNiCrMnMoOOH/NF, FeNiCrMnCeOOH/NF and FeNiCrMnCoOOH/NF.

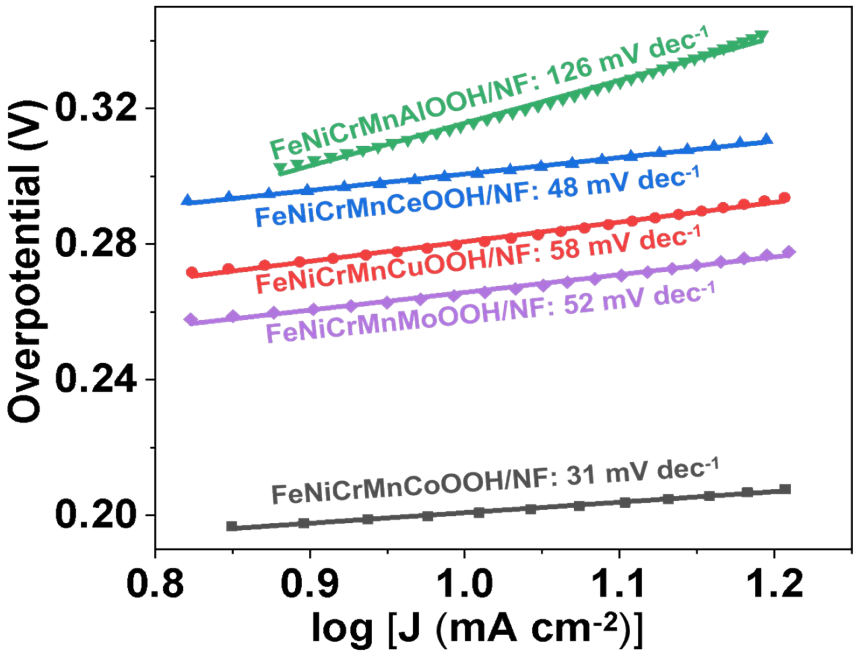

Fig. S6. Tafel slopes of FeNiCrMnAlOOH/NF, FeNiCrMnCuOOH/NF, FeNiCrMnMoOOH/NF, FeNiCrMnCeOOH/NF and FeNiCrMnCoOOH/NF.

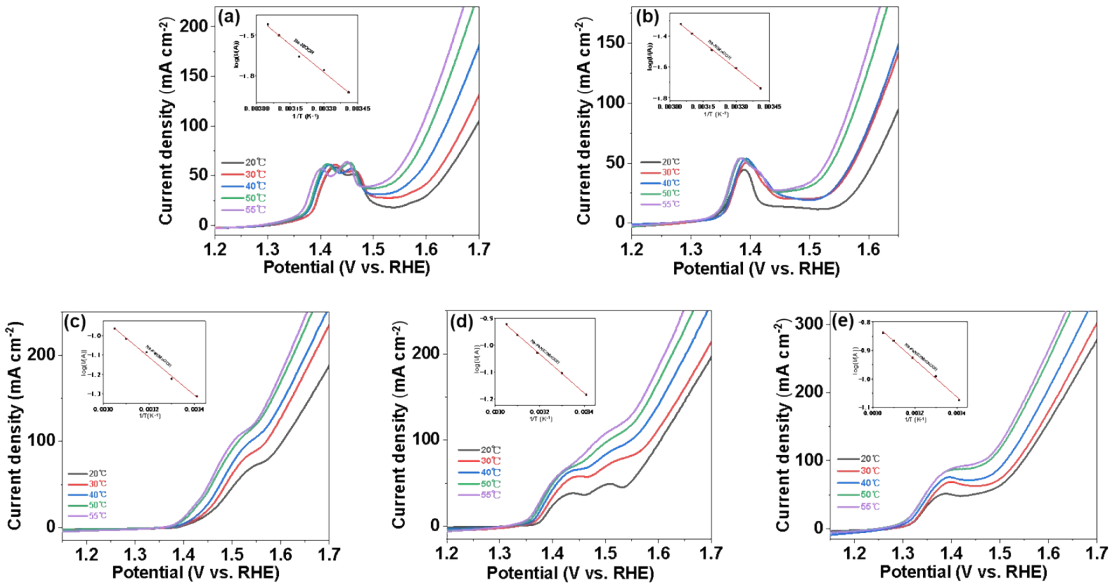

Fig. S7. OER polarization curves of NiOOH/NF, NiMnOOH/NF, FeNiMnOOH/NF, FeNiCrMnOOH/NF and FeNiCrMnCoOOH/NF in three-electrode configuration in 1 M KOH at 20 °C, 30 °C, 40 °C, 50 °C and 55 °C.

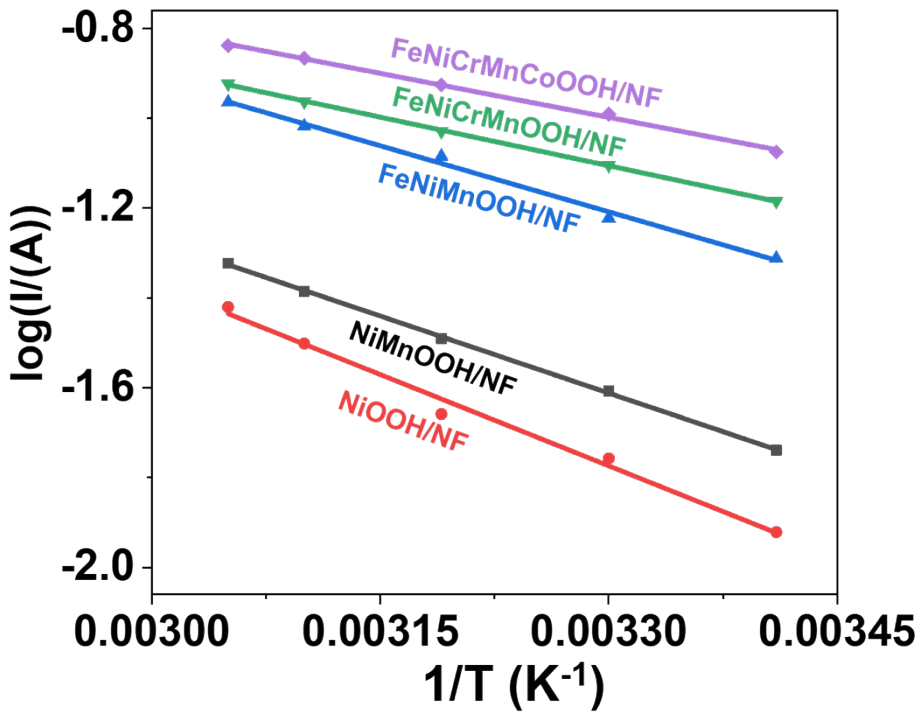

Fig. S8. Arrhenius plots.

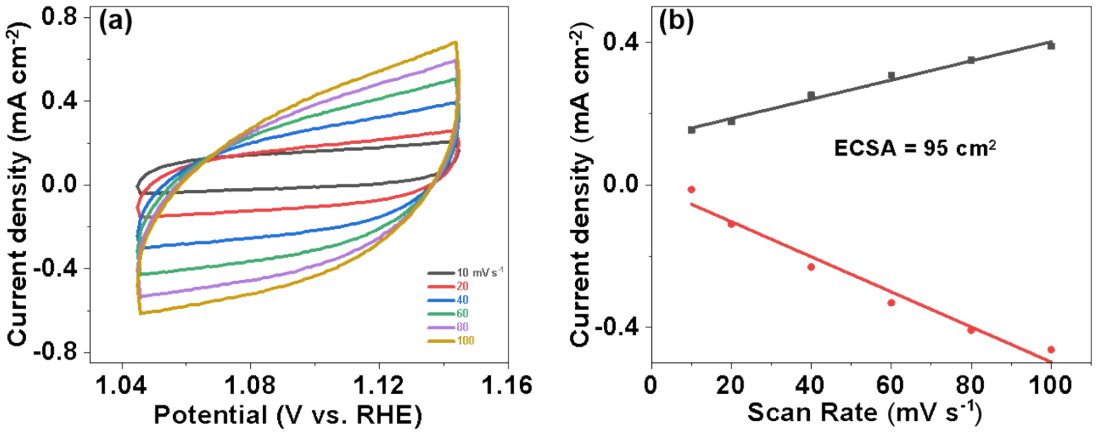

Fig. S9. (a) CVs of the FeNiCrMnCoOOH/NF measured in a non-Faradaic region at different scan Rate. (b) The cathodic and anodic currents measured as a function of the scan Rate.

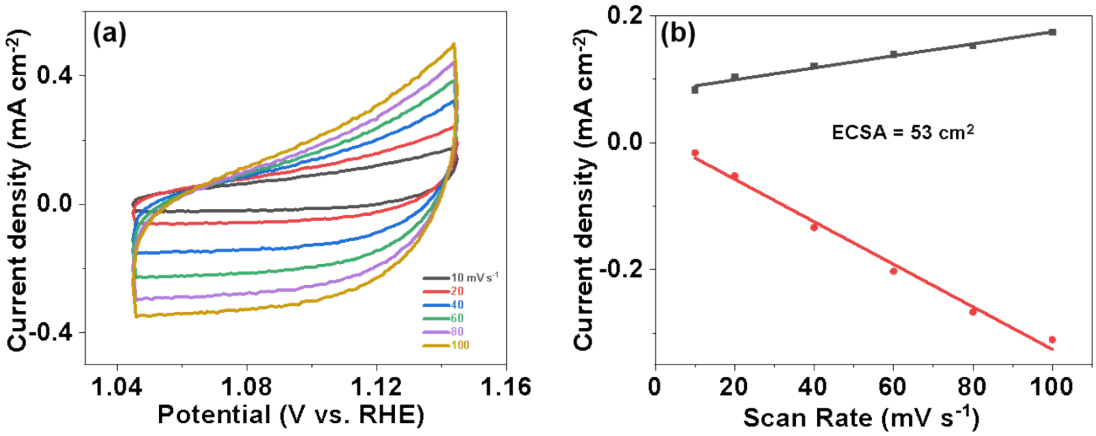

Fig. S10. (a) CVs of the NiOOH/NF measured in a non-Faradaic region at different scan Rate. (b) The cathodic and anodic currents measured as a function of the scan Rate.

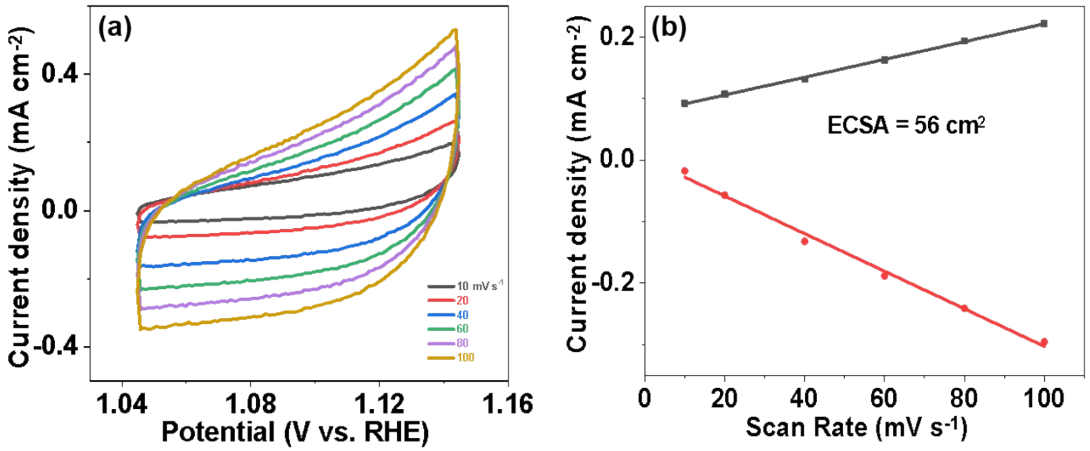

Fig. S11. (a) CVs of the NiMnOOH/NF measured in a non-Faradaic region at different scan Rate. (b) The cathodic and anodic currents measured as a function of the scan Rate.

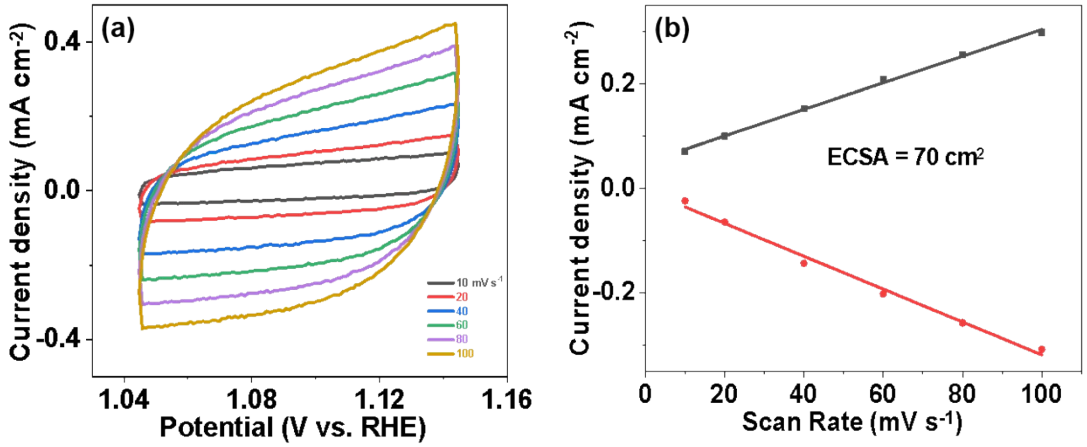

Fig. S12. (a) CVs of the FeNiMnOOH/NF measured in a non-Faradaic region at different scan Rate. (b) The cathodic and anodic currents measured as a function of the scan Rate.

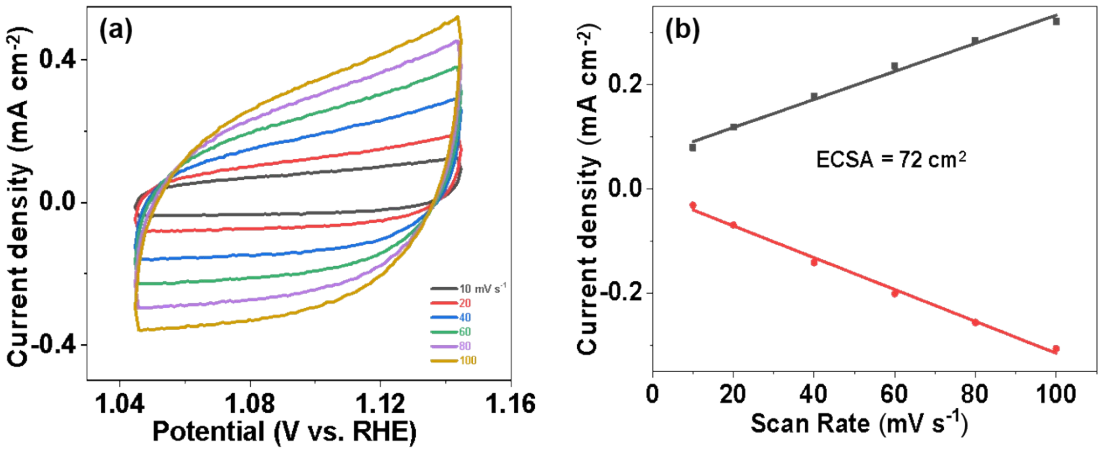

Fig. S13. (a) CVs of the FeNiCrMnOOH/NF measured in a non-Faradaic region at different scan Rate. (b) The cathodic and anodic currents measured as a function of the scan Rate.

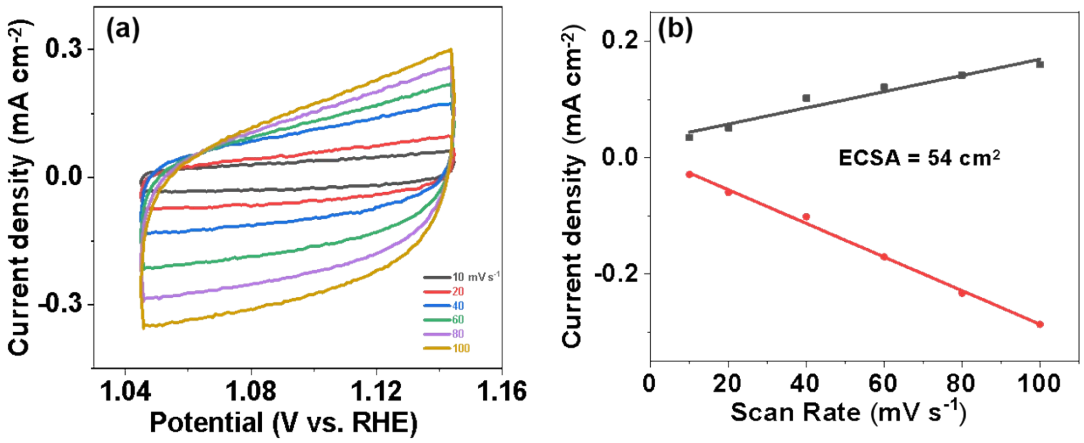

Fig. S14. (a) CVs of the FeNiCrMnAlOOH/NF measured in a non-Faradaic region at different scan Rate. (b) The cathodic and anodic currents measured as a function of the scan Rate.

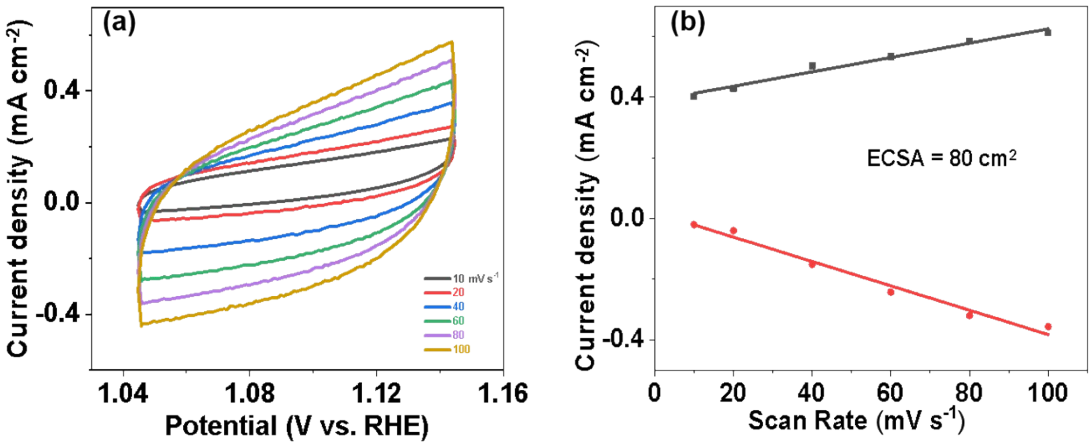

Fig. S15. (a) CVs of the FeNiCrMnCuOOH/NF measured in a non-Faradaic region at different scan Rate. (b) The cathodic and anodic currents measured as a function of the scan Rate.

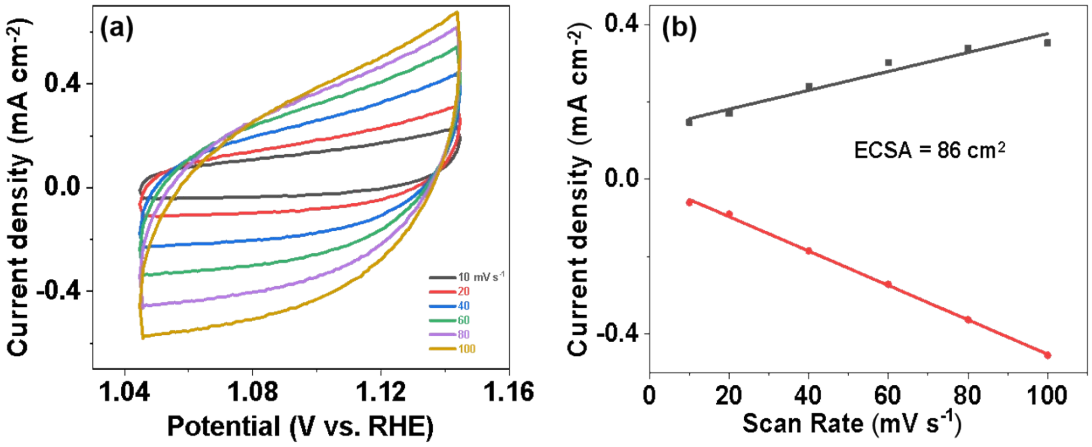

Fig. S16. (a) CVs of the FeNiCrMnMoOOH/NF measured in a non-Faradaic region at different scan Rate. (b) The cathodic and anodic currents measured as a function of the scan Rate.

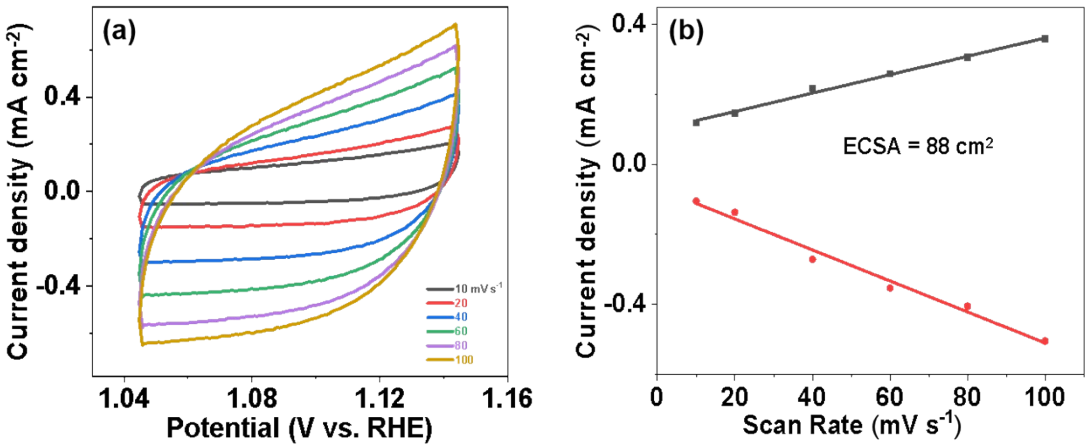

Fig. S17. (a) CVs of the FeNiCrMnCeOOH/NF measured in a non-Faradaic region at different scan Rate. (b) The cathodic and anodic currents measured as a function of the scan Rate.

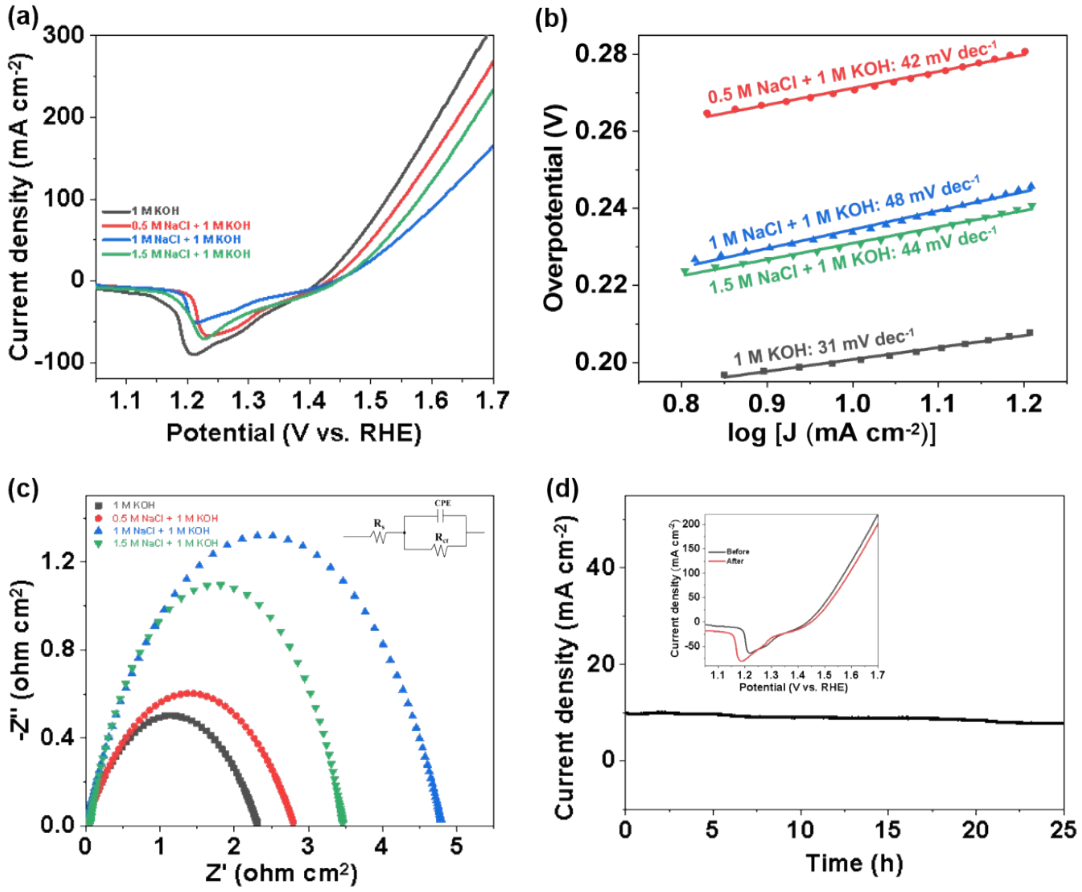

Fig. S18. (a) Electrochemical analysis in alkaline seawater. (b) Tafel slopes. (c) EIS plots (inset: equivalent circuit model corresponding to EIS data). (d) Chronoamperometric curves of the FeNiCrMnCoOOH/NF in 0.5 M NaCl + 1 M KOH.

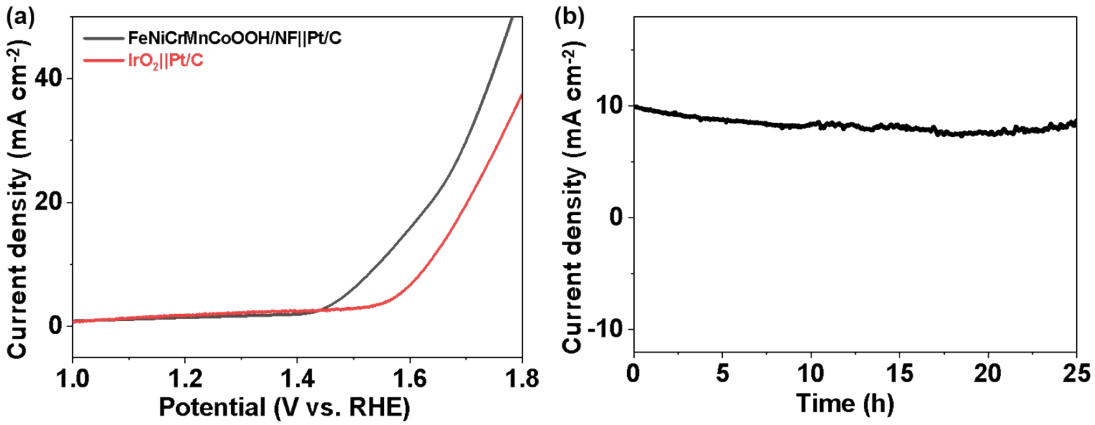

Fig. S19. (a) LSV curves of FeNiCrMnCoOOH/NF||Pt/C and IrO_2||Pt/C of overall water splitting. (b) Stability test.

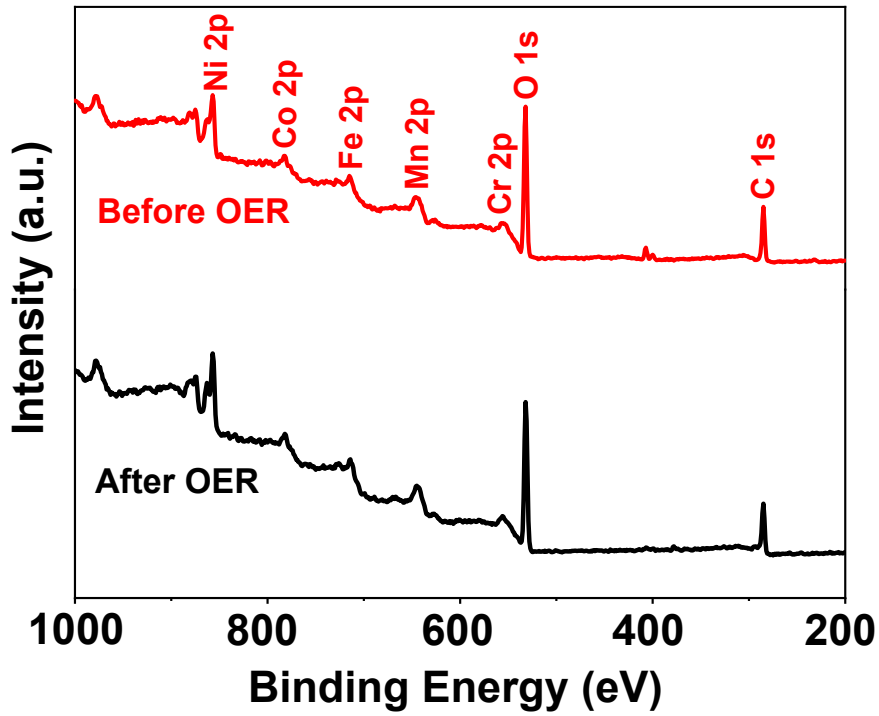

Fig. S20. XPS survey spectra of FeNiCrMnCoOOH/NF (before and after OER test).

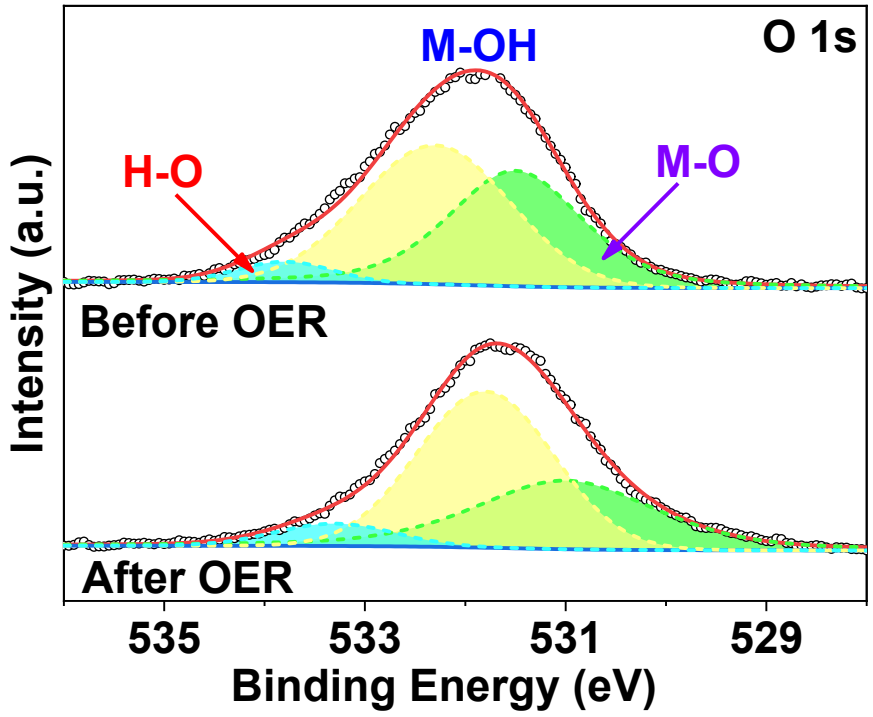

Fig. S21. High-resolution XPS spectrum for O 1s (before and after OER test).

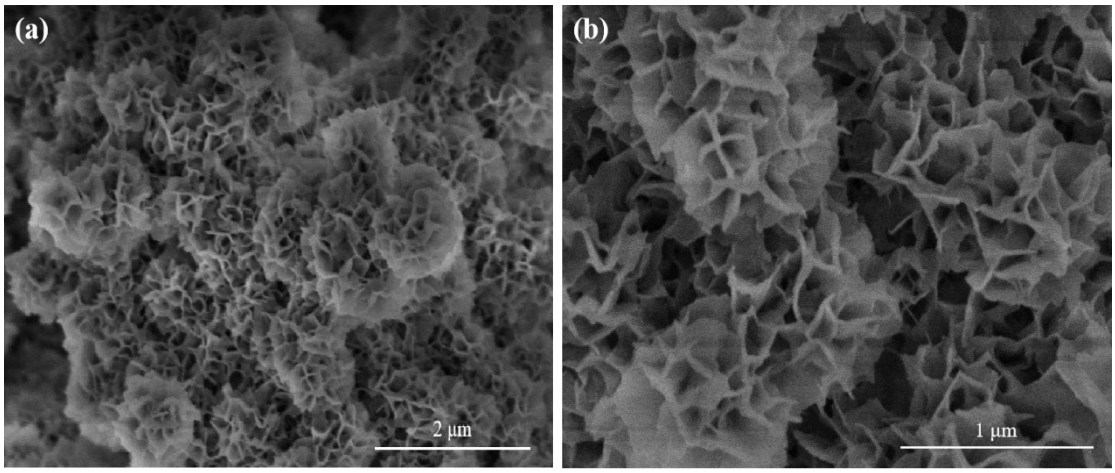

Fig. S22. (a, b) SEM images of FeNiCrMnCoOOH/NF after OER testing.

Table S1. Chemical composition of FeNiCrMnCoOOH/NF.

catalyst	Content (mol%)				
	Fe	Ni	Cr	Mn	Co
FeNiCrMnCoOOH/NF	19.82%	22.36%	20.44%	18.95%	18.43%

Table S2. Comparison of OER performance of FeNiCrMnCoOOH/NF with other (oxy)hydroxides in 1 M KOH

Catalyst	η@10 mA cm^{-2}（mV）	Tafel slope（mV dec^{-1}）	Ref.
FeNiCrMnCoOOH/NF	201	31	This work
Fe(Ni)OOH	300	34	[1]
Te/FeNiOOH-NC	220	52	[2]
(Fe,Co)OOH/MI	230	73	[3]
$(Ni_7Fe_3)OOH$-S	238	42.7	[4]
Fe-Co-OOH/Ni	250	40.28	[5]
S-(Fe/Ni)OOH@NiNCAs-SSM	245	65	[6]
$Fe(Cr)OOH/Fe_3O_4$/NF	198	34	[7]
γ-MnOOH/CoOOH-0.1	313	87	[8]
NiOOH@CoCu CH	263	43.2	[9]
FeNi-CoOOH NSs/CFC	247	42.7	[10]
Co_3O_4-CoOOH/CP	245	68.8	[11]
Mo-NiOOH	310	68	[12]

References

1 D. Tang, O. Mabayoje, Y. Q. Lai, Y. X. Liu and C. B. Mullins, *Chemistryselect*, 2017, **2**, 2230-2234.

2 S. Ibraheem, X. T. Li, S. S. A. Shah, T. Najam, G. Yasin, R. Iqbal, S. Hussain, W. Y. Ding and F. Shahzad, *ACS Appl. Mater. Inter.*, 2021, **13**, 10972-10978.

3 W. Z. Huang, J. T. Li, X. B. Liao, R. H. Lu, C. H. Ling, X. Liu, J. S. Meng, L. B. Qu, M. T. Lin, X. F. Hong, X. B. Zhou, S. L. Liu, Y. Zhao, L. Zhou and L. Q. Mai, *Adv. Mater.*, 2022, **34**, 2200270.

4 W. Liu, X. T. Wang, F. Wang, X. L. Liu, Y. Zhang, W. T. Li, Y. Z. Guo, H. Y. Yin and D. H. Wang, *Chem. Eng. J.*, 2023, **454**, 140030.

5 P. C. Wang, Z. A. Xu, Y. Q. Lin, L. Wan and B. G. Wang, *ACS Sustain. Chem. Eng.*, 2020, **8**, 8949-8957.

6 M. H. Kahnamouei and S. Shahrokhian, *ACS Appl. Energy Mater.*, 2021, **4**, 10627-10638.

7 L. Li, G. W. Zhang, B. Wang and S. C. Yang, *Appl. Catal., B*, 2022, **302**, 120847.

8 M. L. Cui, H. H. Zhao, X. P. Dai, Y. Yang, X. Zhang, X. B. Luan, F. Nie, Z. T. Ren, Y. Dong, Y. Wang, J. T. Yang and X. L. Huang, *ACS Sustain. Chem. Eng.*, 2019, **7**, 13015-13022.

9 B. Li, K. F. Wang, J. X. Ren and P. Qu, *New J. Chem.*, 2022, **46**, 7615-7625.

10 N. Ma, C. C. Gong, H. A. Xie, C. S. Shi, J. W. Sha, C. N. He, F. He, N. Q. Zhao and E. Z. Liu, *Int. J. Hydrogen Energy*, 2022, **47**, 29762-29770.

11 L. Yan and B. Zhang, *Int. J. Hydrogen Energy*, 2021, **46**, 34287-34297.

12 Y. S. Jin, S. L. Huang, X. Yue, C. Shu and P. K. Shen, *Int. J. Hydrogen Energy*, 2018, **43**, 12140-12145.